Atmos. Chem. Phys. Discuss., 2, 2557–2586, 2002
www.atmos-chem-phys.org/acpd/2/2557/

Atmospheric Chemistry and Physics Discussions

Factors controlling Arctic denitrification in cold winters of the 1990s

G. W. Mann, S. Davies, K. S. Carslaw, and M. P. Chipperfield

Institute for Atmospheric Science, School of the Environment, University of Leeds, Leeds, UK

Received: 2 November 2002 – Accepted: 16 December 2002 – Published: 18 December 2002

Correspondence to: G. W. Mann (gmann@env.leeds.ac.uk)

Abstract

Denitrification of the Arctic winter stratosphere has been calculated using a 3-D microphysical model for the winters 1994/95, 1995/96, 1996/97 and 1999/2000. Denitrification is assumed to occur through the sedimentation of low number concentrations of large nitric acid trihydrate (NAT) particles, as observed extensively in 1999/2000. We examine whether the meteorological conditions that allowed NAT particles to grow to the very large sizes observed in 1999/2000 also occurred in the other cold winters. The results show that winter 1999/2000 had conditions that were optimum for denitrification by large NAT particles, which are a deep concentric cold pool and vortex. Under these conditions, NAT particles can circulate in the cold pool for several days, reaching several micrometres in radius and leading to a high downward flux of nitric acid. The other winters had shorter periods with optimum conditions for denitrification. However, we find that NAT particles could have grown to large sizes in all of these winters and could have caused significant denitrification. We define the quantity "closed flow area" (the fraction of the cold pool in which air parcel trajectories can form closed loops) and show that it is a very useful indicator of possible denitrification. We find that even with a constant NAT nucleation rate throughout the cold pool, the average NAT number concentration and size can vary by up to a factor of 10 in response to this meteorological quantity. These changes in particle properties account for a high degree of variability in denitrification between the different winters. This large meteorologically induced variability in denitrification rate needs to be compared with that which could arise from a variable nucleation rate of NAT particles, which remains an uncertain quantity in models.

1. Introduction

Extensive denitrification was observed in 1999/2000 by both in situ (Popp et al., 2001) and remote (Santee et al., 2000; Kleinböhl et al., 2002) instruments. Large NAT par-

ACPD

2, 2557–2586, 2002

ticles (10 to 20 μm diameter) at low number concentrations (between 10^{-5} and 10^{-3} cm^{-3}) were measured by the NOAA NO_y instrument aboard the NASA ER-2 aircraft in the 1999/2000 winter Arctic vortex (Fahey et al., 2001; Northway, 2002a). Previous model calculations (Carslaw et al., 2002; Drdla et al., 2002) show that meteorological conditions in the 1999/2000 Arctic vortex allowed NAT particles to grow to the very large sizes that were observed. These large particles can very efficiently denitrify the lower stratosphere on the timescale of a few days (Fahey et al., 2001; Mann et al., 2002; Northway et al., 2002b; Davies et al., 2002).

The large NAT particles observed in the 1999/2000 Arctic vortex constitute the first unambiguous detection of large sedimenting nitric acid-containing particles. These observations, and model simulations of their development, prompt several questions:

1. Could NAT particles have grown to such very large sizes in other winters, or did the 1999/2000 Arctic vortex have unique properties to allow their development? There are no observations from previous Arctic winters to answer this question. For example, the Aerosol Particle Counter of Deshler and Oltmans (1998) has a lower detection limit of 6×10^{-4} cm^{-3}, so would not have been able to detect many of the populations of large particles in 1999/2000. The Forward Scattering Spectrometer Probe (FSSP) instrument detected 13 μm diameter particles in the Arctic stratosphere during January 1989 (Dye et al., 1992) but these cannot be attributed unambiguously to nitric acid particles.

2. How much denitrification could have been caused in 1999/2000 and in other winters by such particle populations? There are observations of denitrification in all of these winters (Rex et al., 1997; Hintsa et al., 1998; Kondo et al., 2000; Dessler et al., 1999; Santee et al., 1999, 2000; Popp et al., 2001; Kleinböhl et al., 2002). Here, we do not compare model simulations with these observations in detail, but establish the potential for denitrification by NAT particles.

3. Thirdly, what are the factors that control denitrification by low number densities of NAT particles? Vortex-scale modelling of denitrification by Mann et al. (2002)

has shown that the dynamics of the Arctic vortex can control denitrification by determining the length of time a NAT particle stays below the NAT equilibrium temperature T_{NAT} (around 195 K). It was shown that the optimum situation for denitrification is a large cold pool that is concentric with the polar vortex. However, the simulations illustrating this sensitivity were only 10 days long and examined a specific set of conditions. Here we perform complete winter simulations of denitrification of the Arctic vortex for the four coldest winters of the 1990s: 1994/95, 1995/96, 1996/97 and 1999/2000.

Several factors may influence the magnitude and extent of denitrification, including nitric acid and water mixing ratios, cold pool vertical depth, cold pool size, minimum temperature, and hydrate particle number concentrations (e.g. Jensen et al., 2002). Variations in all of these factors, except the latter, are present in the meteorological and trace gas initialisation fields used here. In addition, Mann et al. (2002) have shown that the magnitude of denitrification by low number concentrations of large NAT particles depends critically on the colocation of the cold pool and vortex. Under conditions where the vortex and cold pool are concentric, individual NAT particles can be advected around the cold pool for several days, eventually growing to sizes of several micrometres. In contrast, a highly baroclinic vortex, in which the centre of the cold pool is positioned towards the edge of the vortex, means that individual NAT particles experience short periods of low temperature followed by warming and particle evaporation. Dynamical situations that allow a sedimenting particle to remain below the NAT saturation temperature for ~8 days will be optimum for denitrification (Fahey et al., 2001; Mann et al., 2002). This sensitivity to vortex concentricity will decrease as the particle number concentration increases due to the shorter time required for the particles to reach their final size when equilibrium with gas phase HNO_3 is attained (Jensen et al., 2002). The model predictions we show here assume low number concentrations of NAT particles, as observed in winter 1999/2000, so sensitivity to vortex concentricity can be expected.

In Mann et al. (2002) we defined the concentricity of the cold pool and vortex in

terms of the separation of their centroids. In one case study we showed that the calculated vortex-average denitrification fell linearly from some maximum value to zero as the cold pool centroid was moved from the centroid of the vortex to the vortex edge. Here, we show that the cold pool–vortex centroid separation is a useful quantity for understanding the magnitude of denitrification in several recent winters.

2. Description of the model

The model is described fully in Carslaw et al. (2002) and Mann et al. (2002). Briefly, the model consists of a Lagrangian particle model incorporating the formation, advection, growth and sedimentation of several thousand NAT particles coupled to the 3-D Eulerian off-line stratospheric chemical transport model (CTM) SLIMCAT (e.g. Chipperfield, 1999). The model is forced by 6-hourly wind and temperature fields from European Centre for Medium-Range Weather Forecasts (ECMWF) operational analyses, while vertical advection is calculated in isentropic coordinates from heating rates using the MIDRAD radiation scheme (Shine, 1987).

The particle model calculates the change in gas phase HNO_3 concentrations caused by particle growth and evaporation and feeds this back to the CTM part of the model, which then advects the gas phase species. Particle growth is calculated in the microphysical model as in Appendix A taking into account the advection of gas phase HNO_3 and H_2O. The 3-D particle advection and isentropic trace gas advection steps are done at every time step. The Eulerian model produces daily fields of denitrification calculated by comparison with gas phase HNO_3 from a passive run which has the particle sedimentation switched off. The model also incorporates the removal of gas phase nitric acid and water by supercooled ternary solution droplets, which compete with NAT particle growth using the analytical scheme of Carslaw et al. (1995).

The coupled model is initialized each winter in early December with 3-dimensional fields of gas phase nitric acid and water from multi-annual SLIMCAT simulations. These compare well with observations from 1999/2000 and 1996/97 below 700 K.

ACPD
2, 2557–2586, 2002

We use a volume average NAT nucleation rate of 8.1×10^{-10} particles $cm^{-3}s^{-1}$, which has been shown to reproduce very well changes in the particle number concentration observed in the period January to March 2000 (Carslaw et al., 2002). Particles are initialised with a diameter of 0.1 μm. The particle number concentrations produced in the vortex by assuming this nucleation rate (maxima of $\sim 10^{-5} - 10^{-4}$ cm^{-3}) are at the low end of concentrations that can cause denitrification (Jensen et al., 2002).

We use this same nucleation rate in all the winter-long simulations for two reasons. Firstly, a constant nucleation rate allows us to evaluate the importance of meteorological factors in controlling NAT particle evolution and sedimentation in isolation. Secondly, our current understanding of the origin of large NAT particles does not allow a more sophisticated treatment of their formation in a 3-D model (see Knopf et al., 2002). In short, there is no observational evidence to constrain how the nucleation rate might depend on conditions in the vortex. Note that by using a volume average nucleation rate we are not implying that in reality NAT forms homogeneously throughout the NAT-supersaturated region. Particles may be generated in a more localised fashion (e.g. Fueglistaler et al., 2002). Our model calculations therefore describe a situation in which large particles, produced by whatever mechanism, become well distributed through the vortex, as was observed in January to March 2000 (Northway et al., 2002). The implications of this assumption are discussed in the conclusions section of this paper.

3. Winter-long denitrification simulations

Figures 1a, 2a, 3a and 4a show height-time slices of calculated cumulative denitrification for the winters 1994/95, 1995/96, 1996/97 and 1999/2000 as a percentage of the passive nitric acid mixing ratio. The denitrification is shown as a vortex average, taken to be the mean over all grid boxes with equivalent latitude greater than 70°. Equivalent latitude is a vortex-normalized latitude, with the vortex centre having an equivalent latitude of 90° (Nash et al., 1996).

In each figure, alongside the denitrification are also shown a number of related quantities. In b) the area of the NAT-supersaturated region is shown. This is the area where NAT particles can form and grow. In c) the cold pool-vortex centroid separation (normalised by the effective radius of the NAT region) is shown. A normalised centroid separation of 1 means that the centroids of the cold pool and vortex are separated by 1 effective NAT region radius. In d) the number density of NAT particles is shown (calculated as an average at each level over all SLIMCAT grid boxes containing particles). Panel e) shows the evolution of mean particle radius. Finally, f) shows the height-resolved denitrification rate, calculated by considering the NAT particle mass fluxes at each altitude. The mass flux for each NAT particle is calculated from the mass of the particle multiplied by its sedimentation speed, each calculated as in Carslaw et al. (2002). The volume average mass flux for each SLIMCAT grid box is then calculated. The difference between the mass fluxes entering the top of the box and leaving from below gives an indication of the instantaneous denitrification/renitrification which is occurring. Further details of this calculation are given in Appendix B.

3.1. Winter 1999/2000

Denitrification starts in early December, initially mainly above 500 K, but by the end of December the maximum vortex average denitrification is 35%, with significant denitrification extending from 575 K to 450 K. By 20 January 2000, when the first ER-2 observations of large particles and denitrification were made in the SOLVE/THESEO 2000 campaign, the average vortex denitrification had reached over 65% (around 10 ppb) throughout the altitude range 475 to 550 K. Beyond this date, the denitrification increases only a little and the depth of the denitrified region remains approximately constant. A re-nitrified region is also clearly visible (shown as red in Fig. 1a). Descent of the most denitrified part of the vortex air can also be seen in this winter.

In situ measurements of NO_y and HNO_3 aboard the ER-2 aircraft made in mid-March 2000 showed widespread denitrification had taken place over a large alititude range compared with early December 1999 (Popp et al., 2001; Kleinböhl et al., 2002).

Satellite observations of HNO_3 at 465 K also showed that the denitrification persisted long after temperatures rose above the PSC threshold in early March 2000 (Santee et al., 2000). The denitrification predicted by the model is consistent with both these observations although a detailed comparison has yet to carried out.

The evolution of substantial modeled denitrification can be related to the NAT area and centroid separation. The NAT area is very large over much of the vortex for about 30 days between 15 December and 15 January and the vortex and cold pool also remain close to concentric over much of the altitude range for the same period (indicated by the low values of centroid separation in Fig 1 c). In other words, during this mid-winter period the vortex is concentric whenever temperatures are low and the concentric state of the vortex extends from around 475 K to 600 K. After 15 January the vortex becomes more disturbed and the cold pool-vortex centroid separation increases. It was in this post-January 15 period that all the large nitric acid particle observations were made (Northway et al., 2002a). We have no in situ measurements of the evolution of particle sizes and the magnitude of denitrification in the period 15 December to 15 January when conditions were optimum for growth of NAT particles to large sizes.

Figure 1 also shows altitude-time plots of average NAT particle number concentration N (graph d) and mean NAT particle radius $\bar{r}$ (graph e). The largest particles are found in the lowest part of the cold pool where they have had time to grow to larger sizes from their initial nucleation height. Particles at greater altitudes have, on average, not been growing for as long. The model predicts that large NAT particles were present somewhere in the Arctic throughout late December and most of January in the potential temperature range 350 to 450 K. Average number densities peaked at around 2×10^{-4} cm^{-3} at around 475 K on 12 January 2000 and were consistently of the order 10^{-4} cm^{-3} between 450 and 550 K in the periods 20–30 December 1999 and around 7–20 January 2000.

Panel f) shows the height-resolved denitrification rate. The levels where denitrification and renitrification are occurring at any one time are clearly apparent (coloured blue and red respectively). The vast majority of denitrification took place in December and

January. Denitrification is predicted to have been close to saturation (i.e. gas phase HNO_3 will have approached the HNO_3 vapour pressure over NAT) in much of the vortex by the time the first in situ observations were made on 20 January 2000.

3.2. Winter 1994/95

The dynamical structure of the 1994/95 vortex is quite different to that of the 1999/2000 winter. Figure 2 shows that the area of NAT supersaturation was generally smaller (in both horizontal and vertical extents) than in 1999/2000. The greatest NAT areas were at lower altitudes. The greatest contrast to the 1999/2000 winter is apparent in the centroid separation. Although there are two short periods with a highly concentric cold pool and vortex (13–20 December and 10–15 January) the vortex is generally much more disturbed, with the cold pool centre displaced away from the centre of the vortex. Mann et al. (2002) showed that such a configuration of the cold pool and vortex reduces the rate of denitrification since particles tend to be advected out of the NAT region before they can grow large enough to sediment rapidly.

Denitrification in the model begins after 20 December (after the period of small centroid separation), but increases much more slowly than during the 1999/2000 winter. The predicted vortex-average denitrification reaches a maximum of around 50% (around 8 ppb) in a much thinner layer than in 1999/2000 and denitrification is typically lower at around 30–40%, both of which are consistent with the effect outlined above. Although conditions were not optimum for denitrification for much of winter 1994/95, the model still predicts NAT particle populations similar to those observed during 1999/2000 for the two episodes in December 1994 and January 1995 described above.

3.3. Winter 1995/96

The 1995/96 winter was very cold at high altitudes (> 500 K) with the cold pool reasonably concentric with the vortex (see Fig. 3b) at these altitudes. However, below 500 K

the cold pool centroid was displaced almost to the vortex edge for most of December and January. These periods of high centroid separation coincide with periods of lower NAT areas, and therefore higher temperatures. Significant denitrification is predicted to start only in January 1996, with the peak of the denitrifed layer being above 500 K. The vortex average denitrification reaches a maximum of about 25% (around 4 ppb) at 500 K in January. Only in early February do the vortex and cold pool become nearly concentric over a large altitude range, leading to a further intensification of denitrification to a maximum of around 45% vortex average (around 8 ppb) at 450 K.

3.4. Winter 1996/97

The 1996/97 winter did not get sufficiently cold to form PSCs until January but stayed very cold well into March, much later than in the other winters (see Fig. 4). In mid to late January, there was quite a large and deep area of NAT supersaturation, but the cold pool was not very concentric with the vortex, so particle number density and mean radius both stayed relatively low giving low downward HNO_3 flux and only a small amount of denitrification. By contrast, in February the centroid separation was low, meaning a concentric vortex and cold pool. Between days 35 and 60, this arrangement allowed NAT particles to reach large sizes and to accumulate relatively high number densities causing the region between 430 and 490 K to become more than 30% denitrified by the beginning of March.

3.5. Overview

The model calculates moderate to large denitrification in some areas of the Arctic stratosphere for all these four cold winters of the 1990s (see Table 1). In addition, large NAT particles are predicted to occur in each winter. Average number concentrations of particles reach a maximum of about 10^{-4} cm^{-3}, but vary greatly during each winter. Winter 1999/2000 has the highest average number concentrations ($\sim 2 \times 10^{-4}$ cm^{-3}), although these occurred before the ER-2 in situ observations (Fahey et al., 2001).

ACPD
2, 2557–2586, 2002

Figure 5 shows histograms of the calculated denitrification on the 475 K level on 28 February for each of the years. These give an indication of the variation of the denitrification about the mean. There is great variability in the magnitude and range of denitrification in the vortex. Winter 1994/95 shows moderately denitrified air with a narrow range while winter 1996/97 has a bimodal distribution of denitrification, with some air being only slightly denitrified and other air being quite strongly denitrified. This bi-modal distribution reflects the late and intensive occurrence of denitrification in the 1996/97 winter. Winter 1999/2000 has the strongest and most widespread denitrification at this time and altitude.

4. Factors controlling denitrification

4.1. What the simulations tell us

These model simulations show that a number of factors control the magnitude of denitrification by low number concentrations of NAT particles. Denitrification depends on the development of populations of large NAT particles over several days. These particles grow, sediment, and are advected by the wind over several days, so the dependence of denitrification on meteorology is therefore complex.

An examination of Figs. 1–4 suggests that during some periods the cold pool area is a good indicator of denitrification rate (panel f), while at other times the cold pool-vortex centroid separation is better. For example, cold pool area appears to drive the denitrification rate between days 40 and 60 in 1996/97 (Fig. 4) during a period with low centroid separation. In contrast, the centroid separation seems to drive the denitrification rate between days 35 and 45 in 1995/96 (Fig. 3).

Figure 6 shows this latter period in more detail. On day 35 a reasonably large NAT-supersaturated region forms which is concentric with the polar vortex. On day 41, this region begins to get larger and deeper to a maximum on day 44. However, as it does so, its centre moves towards the edge of the polar vortex (the centroid separation in-

ACPD
2, 2557–2586, 2002

creases) and consequently the particle number density reduces by around 50% and the mean radius also reduces significantly. The lowest panel shows how, in this instance, the denitrification is controlled by the concentricity of the vortex despite the increase in the size of the cold pool.

Note that neither the cold pool area nor the centroid separation would control the denitrification rate in a model in which the particles were in equilibrium with the gas phase (Mann et al., 2002). The denitrification rate in panel f is calculated as per unit area of the cold pool, so making the cold pool bigger does not influence this rate (although it would of course, if calculated as a vortex average). The dependence of denitrification rate on cold pool area and centroid separation therefore reflects a sensitivity to Arctic meteorology arising from the time-dependent growth of the NAT particles.

4.2. Concept of "closed-flow" and "through-flow" as indicators of potential denitrification

The cold pool area and the concentricity of the cold pool and vortex both act together to control the temperature trajectories of the particles. The dependence of the denitrification rate on the centroid separation is clear: Mann et al. (2002) showed that a concentric cold pool and vortex allows particles to grow over several days, reaching large sizes and inducing a high downward HNO_3 flux. Thus, a concentric cold pool and vortex create regions of "closed flow" in which particles can circulate in the cold pool for several days. The reason for the dependence of the denitrification rate on cold pool area is not so immediately obvious. It arises because the size of the cold pool also determines the region of the cold pool with closed flow.

Figure 7 shows schematically how the cold pool-vortex concentricity and the cold pool area control denitrification. In (a) an inititially concentric cold pool and vortex creates a large region of closed flow (shaded region) in which particles can circulate for several days and grow to large sizes. As the cold pool (with constant size) is shifted away from the vortex centre, the region of closed flow shrinks. Panel (b) shows that maintaining a fixed relative position of the cold pool and vortex but reducing the cold

pool size also has the effect of reducing the area with closed flow.

The potential for denitrification is a maximum in the region of closed flow and, although not zero, the rate of denitrification is likely to be much lower in the "flow-through" region where NAT particles can grow for a shorter time. The denitrification rate depends in a very non-linear way on the time available for growth, t (Carslaw et al., 2002). The particle mass increases with $t^{3/2}$ and the fall distance increases with t^2. In addition, assuming a constant nucleation rate, particle number concentrations will increase with t. This equates to a very strong dependence of denitrification rate on the time available for growth, such that the closed flow region will dominate denitrification.

We can test this hypothesis by plotting the height-resolved denitrification rate against the fraction of the cold pool that is in closed flow. This fraction, c_{flow} is calculated as follows

$$c_{flow} = \frac{(r_{cp} - c)^2}{r_{cp}^2}, \quad (1)$$

where r_{cp} is the cold pool radius and c is the separation of the cold pool and vortex centroids. Note that this fraction of the cold pool with closed flow assumes circle-equivalent radii. Figure 8 shows a plot of the mean of this denitrification rate against the mean of c_{flow} in the denitrifying region of the cold pool (i.e. ignoring areas of renitrification). Points are shown for all 4 winters for each day where a NAT region existed. Also shown is a line plot indicating the mean and standard deviation of the denitrification rate for bins of closed flow fraction of width 0.05. The y value of each point is the denitrification rate calculated with a 3 day time lag relative to the x axis. The existence of this time lag can be seen from the tilt evident in the instantaneous denitrification rate plots in Figs. 6d, e and f.

Although there is a large amount of scatter in the plot, the overall pattern is clear. For situations where the cold pool is mainly in closed flow, the denitrification rate is much higher than more disturbed situations. Only the region of the cold pool in closed flow has conditions conducive to the production of large NAT particles which are efficient

ACPD
2, 2557–2586, 2002

at denitrification. The mean height-resolved denitrification rate for periods in which all cold pool air is in through flow (i.e. no closed flow in the cold pool) is 0.026×10^{-12} $kgm^{-2}s^{-1}$, a factor of 10 lower than when more than half of the cold pool is in closed flow.

A number of factors have combined to cause the large scatter in Fig. 8. Firstly, in years of strong denitrification, areas of the vortex develop containing a very low mixing ratio of HNO_3. Consequently, although the cold pool may be large and be mostly in closed flow, there may be no supply of HNO_3 available to form the large NAT particles and the denitrification will be lower than expected. This is the case for the blue triangles (from 1999/2000) in Fig. 8 which appear to have anomalously low denitrification rates when the closed flow fraction is high. The wide extent of strong denitrification in that winter meant that by mid-January, a significant portion of the vortex was more than 80 % denitrified. Secondly, when the vortex becomes elongated, the actual closed-flow area can be significantly smaller (or larger) than predicted by assuming circular geometry. This introduces further scatter in the plot. Thirdly, as we have seen, the fraction of cold pool which has closed flow can vary in complicated ways in the vertical, hence a straightforward mean in the vertical adds further scatter. Fourthly, the timescale of dynamical changes in the vortex is similar to the timescale of changes in particle sizes and number concentrations. It takes around 8 days for a steady particle population to be generated (Carslaw et al., 2002; Mann et al., 2002) so any change in the vortex-cold pool arrangement during that time can complicate the relationship between closed flow area and denitrification rate even further. Future studies could perhaps examine the actual area of closed flow derived from the flow fields, rather than using an assumption of circular geometry for the cold pool and vortex.

The rather complicated dependence of denitrification rate on vortex dynamics means that denitrification is not easy to parameterise. A large area of closed flow in the cold pool is a pre-requisite for rapid denitrification, but the actual rate of denitrification can be reduced by a number of factors. However, it is worth noting again, that as shown in Mann et al. (2002) an increase in denitrification rate with closed flow fraction would

ACPD
2, 2557–2586, 2002

not be reproduced in a model that assumed equilibrium between the particles and the gas phase. This is an additional sensitivity that arises from the non-linear growth and sedimentation behaviour of the particles. The *vortex*-average denitrification will depend additionally on the fraction of the vortex with temperatures below T_{NAT}, but this will be a linear dependence.

5. Conclusions

Our analysis shows that denitrification could have occurred in previous cold winters with low volume-average NAT nucleation rates similar to those derived for winter 1999/2000. However, the magnitude of denitrification in winter 1999/2000 was significantly greater than in many previous cold winters because the vortex dynamics were optimum. These optimum conditions are a deep cold pool positioned towards the centre of the vortex, which allows for long NAT particle lifetimes. Long lifetimes allow particles to reach large sizes, which increases their fall speed (proportional to radius squared) as well the amount of nitric acid sequestered in the particles. In addition, the dynamical conditions that lead to long particle lifetimes also allow particles to accumulate in the cold pool over several days, while shorter lifetimes are consistent with a higher loss rate of particles. Thus, particle number concentration, size, and fall speed (and hence downward HNO_3 flux) are all increased when the cold pool and vortex are concentric.

The reliability of the calculated denitrification depends primarily on the assumption of a constant volume-average NAT particle formation rate in each of the four winters. We have assumed that some process, as yet unidentified, generates low number concentrations of NAT particles throughout the NAT supersaturated region. The constant NAT formation rate that we have used produces particle number densities in good agreement with observations over a 2 month period during winter 2000 (Carslaw et al., 2002). This good agreement suggests that much of the variability in particle populations (and hence denitrification) might be controlled by the subsequent vortex-scale evolution of particles after formation, rather than just by the nucleation rate. Particle evolution is

well treated in our model, being controlled largely by the variable dynamic structure of the polar vortex, cold pool location, etc. These processes alone give rise to a large degree of variability in particle populations and denitrification rate in different winters, and even within a single winter. An example of this was described in Sect. 4.1. Any meteorologically induced variation in nucleation rate will add to this variablility.

Although our volume-average formation mechanism produces good agreement with particle concentrations and sizes wherever these were observed, it should be noted that it also produces particles where none were observed. Further comparisons with observations of the type undertaken by Carslaw et al. (2002) need to be undertaken to see whether an alternative particle formation mechanism can significantly improve on the simple scheme we have so far used. Such comparisons should also be extended to winters other than 1999/2000 in light of the uniqueness of this winter identified here.

An analysis of Arctic vortex concentricity for 10 winters (1984/85 to 1993/94) by Pawson et al. (1995) shows that highly concentric vortices occur for at least a short period in most cold winters, although not always synchronous with the lowest temperatures. During this 10 year period, 1988/89 and 1989/90 stand out as potentially vulnerable to denitrification similar to that observed in 1999/2000, since they had long periods of low temperatures with a concentric vortex. Indeed, Fahey et al. (1990) observed significant denitrification of the Arctic in February 1989. Examination of the Pawson et al. (1995) analyses and inclusion of more recent observations suggests that optimum conditions for intense Arctic denitrification occur about 3 times per decade.

Finally, we have defined a quantity which we call the “closed-flow area” that is a good indicator of likely denitrification. The closed-flow area, or fraction of the cold pool in which air parcels form closed loops, captures simultaneously the sensitivity of modelled denitrification to cold pool area and cold pool–vortex concentricity. Our calculations show that the denitrification rate increases substantially as soon as some of the cold pool contains air in closed flow.

Our simulations demonstrate that previous cold Arctic winters were susceptible to denitrification by low number concentrations of NAT particles. We have also identified

meteorological factors that control the denitrification rate. Further investigations are required to test these model simulations against observations during past and future Arctic winters.

Appendix A: Particle growth in the microphysical model

Particle growth is calculated in the microphysical model as in Carslaw et al. (2002) by comparing the ambient HNO_3 partial pressure p_{HNO_3} with the saturation HNO_3 vapour pressure over NAT $p^{NAT}_{HNO_3}$:

$$\frac{dr}{dt} = \frac{G}{r}, \tag{A1}$$

$$G = \frac{D^*_{HNO_3} M_{NAT}}{\rho_{NAT} RT} \left(p_{HNO_3} - p^{NAT}_{HNO_3} \right). \tag{A2}$$

The modified diffusion coefficient $D^*_{HNO_3}$ is given by

$$D^*_{HNO_3} = \frac{D_{HNO_3}}{1 + 4D_{HNO_3}/(\overline{c}_{HNO_3} r)}, \tag{A3}$$

where D_{HNO_3} is the diffusion coefficient of HNO_3 in air and $\overline{c}_{HNO_3}$ is the mean molecular speed. The expression of Hanson and Mauersberger (1988) is used to calculate $p^{NAT}_{HNO_3}$.

Appendix B: Calculation of height-resolved denitrification rate

The height-resolved rate of denitrification in each grid box is calculated as the difference in mass flux of NAT falling into and out of that grid box. The NAT mass flux is first

calculated in each grid box as the sum over all particles of mass m in the grid box multiplied by their fall velocity w_f.

$$m(r) = \frac{4}{3}\pi\rho_{NAT}r^3 \tag{B1}$$

$$w_f(r,T,p) = \left(\frac{2g\rho_{NAT}C_C}{9\nu}\right)r^2 \tag{B2}$$

where ρ_{NAT} is the NAT crystal mass density = 1.6×10^3 kgm^{-3}, C_C is the Cunningham slip correction factor,

$$C_C = 1 + \frac{\lambda}{r}\left[1.257 + 0.4\exp\left(\frac{-1.1r}{\lambda}\right)\right], \tag{B3}$$

where λ is the mean free path of HNO_3 molecules. The volume-averaged mass flux (per unit area) F_{NAT} in kgm^{-2}s^{-1} at each θ level is then found by taking the sum of the grid box mass fluxes divided by the total grid box volume containing NAT particles. The height-resolved denitrification rate $\frac{dM}{dt}$ is then calculated on each day as the difference between the inward and outward mass fluxes

$$\frac{dM}{dt} = \frac{F_{NAT}(\theta_{j-1})A_{NAT}(\theta_{j-1}) - F_{NAT}(\theta_{j+1})A_{NAT}(\theta_{j+1})}{A_{NAT}(\theta_j)} \tag{B4}$$

where A_{NAT} is the area supersaturated with respect to NAT (i.e. where $T < T_{NAT}$).

Acknowledgements. This work was funded by the European Commission, EC, Fifth Framework Program MAPSCORE project, EVK2-CT-2000-00072 and by a NERC studentship.

References

Carslaw, K. S., Luo, B. P., and Peter, T.: An analytic expression for the composition of aqueous HNO_3 - H_2SO_4 stratospheric aerosols including gas-phase removal of HNO_3, Geophys. Res. Lett., 22, 1877–18800, 1995.

Carslaw, K. S., Kettleborough, J., Northway, M. J., Davies, S., Gao, R.-S., Fahey, D. W., Baumgardner, D. G., Chipperfield M. P., and Kleinböhl, A.: A vortex-scale simulation of the growth and sedimentation of large nitric acid particles observed during SOLVE/THESEO 2000, J. Geophys. Res., in press., 2002.

Chipperfield, M. P.: Multiannual simulations with a three-dimensional chemical transport model, J. Geophys. Res., 104, 1781–1805, 1999.

Davies, S., Chipperfield, M. P., Carslaw, K. S., Sinnhuber, B.-M., Anderson, J. G., Stimpfle, R., Wilmouth, D., Fahey, D. W., Popp, P. J., Richard, E. C., Von Der Gathen, P., Jost, H., and Weber, C. R.: Modeling the effect of denitrification on Arctic ozone depletion during winter 1999/2000, J. Geophys. Res., in press, 2002.

Deshler, T. and Oltmans, S. J.: Vertical profiles of volcanic aerosols and polar stratospheric clouds above Kiruna, Sweden: winters 1993 and 1995, J. Atmos. Chem., 30, 11–23, 1998.

Dessler, A. E., Wu, J., Santee, M. L., and Schoeberl, M. R.: Satellite observations of temporary and irreversible denitrification, J. Geophys. Res., 104, 13993–14002, 1999.

Drdla, K., Schoeberl, M. R., and Browell, E. V.: Microphysical modelling of the 1999–2000 Arctic winter: 1. Polar stratospheric clouds, denitrification, and dehydration, J. Geophys. Res., 108, D5, 55–1,21, 2002.

Dye, J. E., Baumgardner, D., Gandrud, B. W., Kawa, S. R., Kelly, K. K., Loewenstein, M., Ferry, G. V., Chan, K. R., and Gary, B. L.: Particle size distributions in Arctic polar stratospheric clouds, growth and freezing of sulphuric acid droplets and implications for cloud formation, J. Geophys. Res., 97, 8015–8034, 1992.

Fahey, D. W., Kelly, K. K., Kawa, S. R., Tuck, A. F., Loewenstein, M., Chan, K. R., and Heidt, L. E.: Observations of denitrification and dehydration in the winter polar stratospheres, Nature, 344, 321–324, 1990.

Fahey, D. W., Gao, R. S., Carslaw, K. S., Kettleborough, J., Popp, P. J., Northway, M. J., Holecek, J. C., Ciciora, S. C., McLaughlin, R. J., Thompson, T. L., Winkler, R. H., Baumgardner, D. G., Gandrud, B., Wennberg, P. O., Dhaniyala, S., McKinney, K., Peter, Th., Salawitch, R. J., Bui, T. P., Elkins, J. W., Webster, C. R., Atlas, E. L., Jost, H., Wilson, J. C., Herman, R. L., Kleinboehl, A., and Von Koenig, M.: The detection of large HNO_3-containing particles in the winter arctic stratosphere and their role in denitrification, Science, 291, 1026–1031, 2001.

Hanson, D. and Mauersberger, K.: Laboratory studies of the nitric acid trihydrate: Implications for the south polar stratosphere, Geophys. Res. Lett., 15, 855–858, 1988.

Hintsa, E. J., Newman, P. A., Jonsson, H. H., Webster, C. R., May, R. D., Herman, R. L., Lair,

L. R., Schoeberl, M. R., Elkins, J. W., Wamsley, P. R., Dutton, G. S., Bui, T. P., Kohn, D. W., and Anderson, J. G.: Dehydration and denitrification in the Arctic polar vortex during the 1995–1996 winter, Geophys. Res. Lett., 25, 501–504, 1998.

Jensen, E., Toon, O. B., Drdla, K., and Tabazadeh, A.: Impact of polar stratospheric cloud particle composition, number density, and lifetime on denitrification, J. Geophys. Res., 107, D20, 27–1,8, 2002.

Kleinböhl, A., Bremer, H., Von Koenig, M., Koellman, H., Kunzi, K. F., Goede, A. P. H., Browell, E. V., Grant, W. B., Toon, G. C., Blumenstock, T., Galle, B., Sinnhuber, B.-M., and Davies, S.: Vortexwide denitrification of the Arctic polar stratosphere in winter 1999/2000 determined by remote observations, J. Geophys. Res., 108, D5, 48–1,11, 2002.

Knopf, D. A., Luo, B. P., Weers U. G., and Peter, T.: Homogeneous nucleation of NAD and NAT in liquid stratospheric aerosols: insufficient to explain denitrification, Atmos. Chem. Phys., 2, 207–214, 2002.

Kondo, Y., Irie, H., Koike, M., and Bodeker, G. E., Denitrification and nitrification in the Arctic stratosphere during winter of 1996–1997: Geophys. Res. Lett., 27, 337–340, 2000.

Mann, G. W., Davies, S., Carslaw, K. S., Chipperfield, M. P., and Kettleborough, J.: Polar vortex concentricity as a controlling factor in Arctic denitrification, J. Geophys. Res., 107, D22, 13–1,11, 2002.

Nash, E. R., Newman, P. A., Rosenfield, J. E., and Schoeberl, M. R.: An objective determination of the polar vortex using Ertel's potential vorticity, J. Geophys. Res., 101, 9471–9478, 1996.

Northway, M. J., Gao, R. S., Popp, P. J., Holecek, J. C., Fahey, D. W., Carslaw, K. S., Tolbert, M. A., Lait, L. R., Dhaniyala, S., Flagan, R. C., Wennberg, P. O., Mahoney, M. J., Herman, R. L., Toon, G. C., and Bui, T. P.: An analysis of large HNO_3-containing particles sampled in the Arctic stratosphere during the winter of 1999–2000, J. Geophys. Res., in press, 2002a.

Northway, M. J., Popp, P. J., Gao, R.-S., Fahey, D. W., Toon, G. C., and Bui, T. P.: Relating inferred HNO_3 flux values to the denitrification of the 1999/2000 Arctic vortex, Geophys. Res. Lett., 29, 63 1–4, 2002b.

Pawson, S., Naujokat, B., and Labitzke, K.: On the polar stratospheric cloud formation potential of the northern stratosphere, J. Geophys. Res., 100, 23215–23225, 1995.

Popp, P. J., Northway, M. J., Holecek, J. C., Gao, R. S., Fahey, D. W., Elkins, J. W., Hurst, D. F., Romashkin, P. A., Toon, G. C., Sen, B., Schauffler, S. M., Salawitch, R. J., Webster, C. R., Herman, R. L., Jost, H., Bui, T. P., Newman, P. A., and Lait, L. R.: Severe and extensive denitrification in the 1999–2000 Arctic winter stratosphere, Geophys. Res. Lett., 28, 2875–

2878, 2001.
Rex, M., Harris, N. R. P., von der Gathen, P., Lehmann, R., Braathen, G. O., Reimer, E., Beck, A., Chipperfield, M. P., Alfier, R., Allaart, M., O'Connor, F., Dier, H., Dorokhov, V., Fast, H., Gil, M., Kyro, E., Litynska, Z., Mikkelsen, I. S., Molyneux, M. G., Nakane, H., Notholt, J., Rummukainen, M., Viatte, P., and Wenger, J.: Prolonged stratospheric ozone loss in the 1995–96 Arctic winter, Nature, 389, 835–838, 1997.
Santee, M. L., Manney, G. L., Froidevaux, L., Read, W. G., and Waters, J. W.: Six years of UARS Microwave Limb Sounder HNO_3 observations: Seasonal, interhemispheric, and interannual differences in the lower stratosphere, J. Geophys. Res., 104, 8225–8246, 1999.
Santee, M. L., Manney, G. L., Livesey, N. J., and Waters, J. W.: UARS Microwave Limb Sounder observations of denitrification and ozone loss in the 2000 Arctic late winter, Geophys. Res. Lett., 27, 3213–2316, 2000.
Shine, K. P.: The middle atmosphere in the absence of dynamical heat fluxes, Q. J. R. Meteorol. Soc., 113, 603–633, 1987.

Table 1. Maximum vortex average denitrification and absolute maximum denitrification in the four cold winters of the 1990s. Also shown are the timing and altitude in each case

	Vortex average denit.			Absolute maximum denit.		
Year	Maximum (%)	Altitude (K)	Timing (Jul. day)	Maximum (%)	Altitude (K)	Timing (Jul. day)
94/95	50	455	17	92	455	2
95/96	52	455	50	78	455	51
96/97	44	455	78	85	465	58
99/00	66	510	21	97	505	21

ACPD
2, 2557–2586, 2002

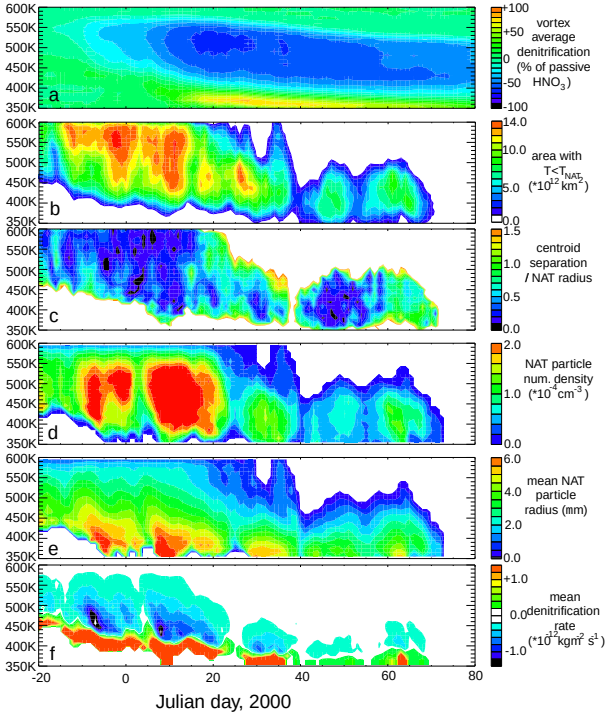

Fig. 1. Altitude-times plots for winter 1999/2000 of **(a)** vortex average denitrification; ((**b)** area of Arctic stratosphere below T_{NAT}; **(c)** normalized centroid separation; **(d)** particle number concentration; **(e)** mean particle radius; and **(f)** height-resolved denitrification rate. Vortex average denitrification is calculated from all grid boxes with equivalent latitude > 70 degrees. Particle number concentration is the mean over all grid boxes containing NAT particles. The centroid separation is normalized by the effective NAT region (cold pool) radius. The denitrification rate is calculated as described in Appendix B.

ACPD
2, 2557–2586, 2002

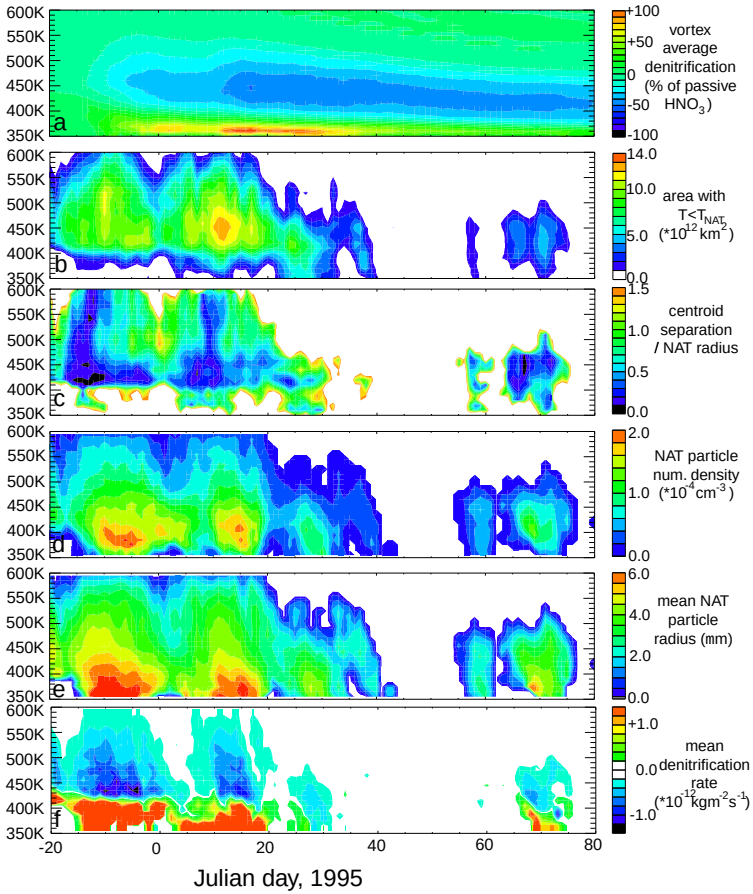

Fig. 2. Altitude time plots for winter 1994/95 of **(a)** vortex average denitrification; **(b)** area of Arctic stratosphere below T_{NAT}; **(c)** normalized centroid separation; **(d)** particle number concentration; **(e)** mean particle radius; and **(f)** denitrification rate.

ACPD
2, 2557–2586, 2002

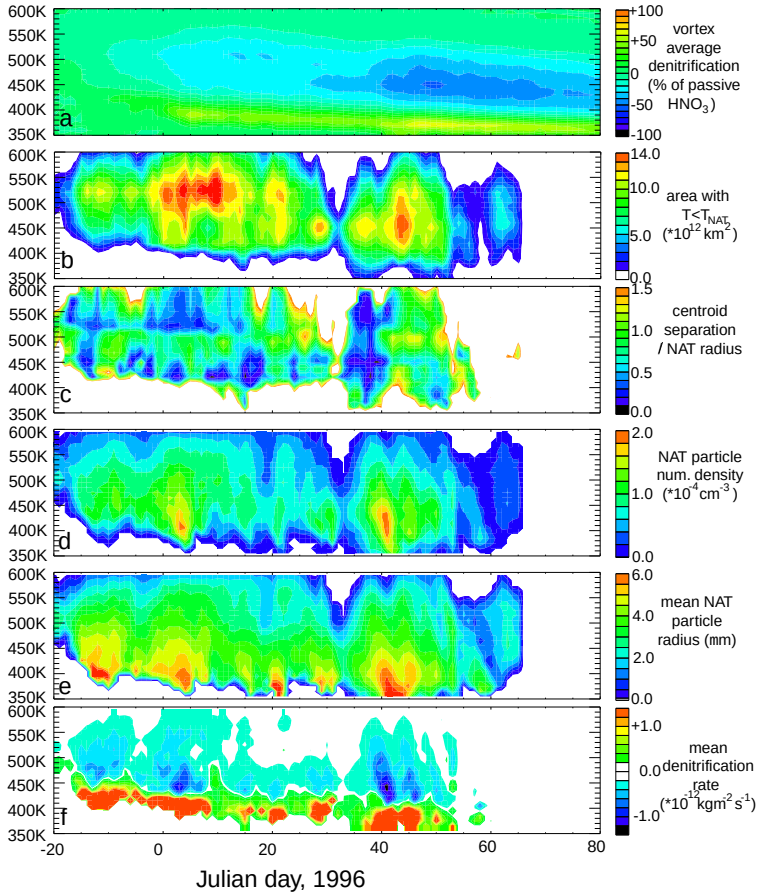

Fig. 3. Altitude time plots for winter 1995/96 of **(a)** vortex average denitrification; **(b)** area of Arctic stratosphere below T_{NAT}; **(c)** normalized centroid separation; **(d)** particle number concentration; **(e)** mean particle radius; and **(f)** denitrification rate.

ACPD
2, 2557–2586, 2002

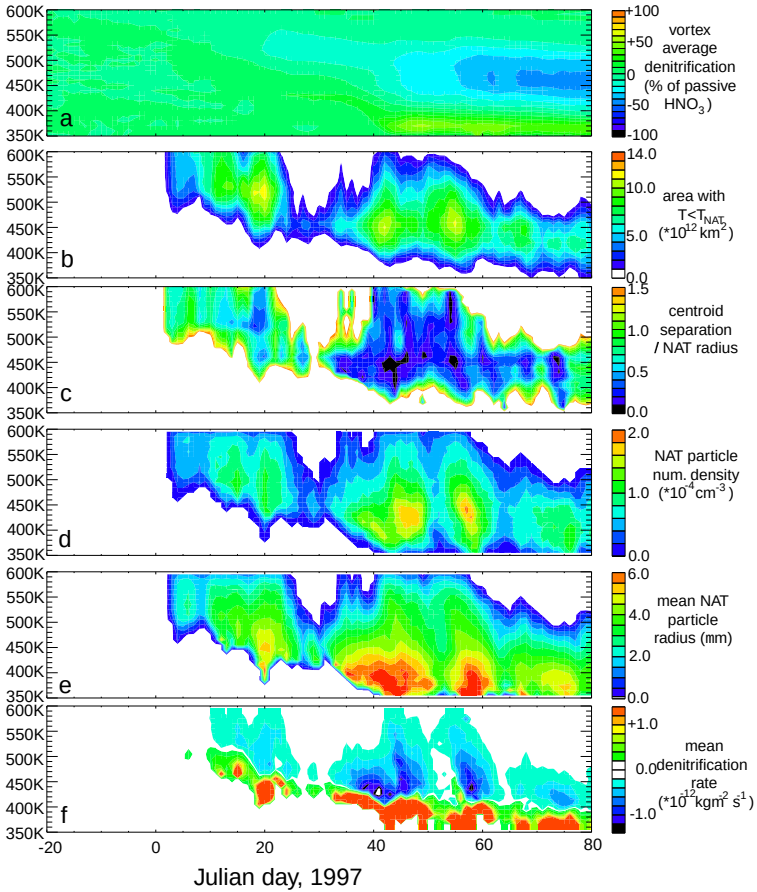

Fig. 4. Altitude time plots for winter 1996/97 of **(a)** vortex average denitrification; **(b)** area of Arctic stratosphere below T_{NAT}; **(c)** normalized centroid separation; **(d)** particle number concentration; **(e)** mean particle radius; and **(f)** denitrification rate.

ACPD
2, 2557–2586, 2002

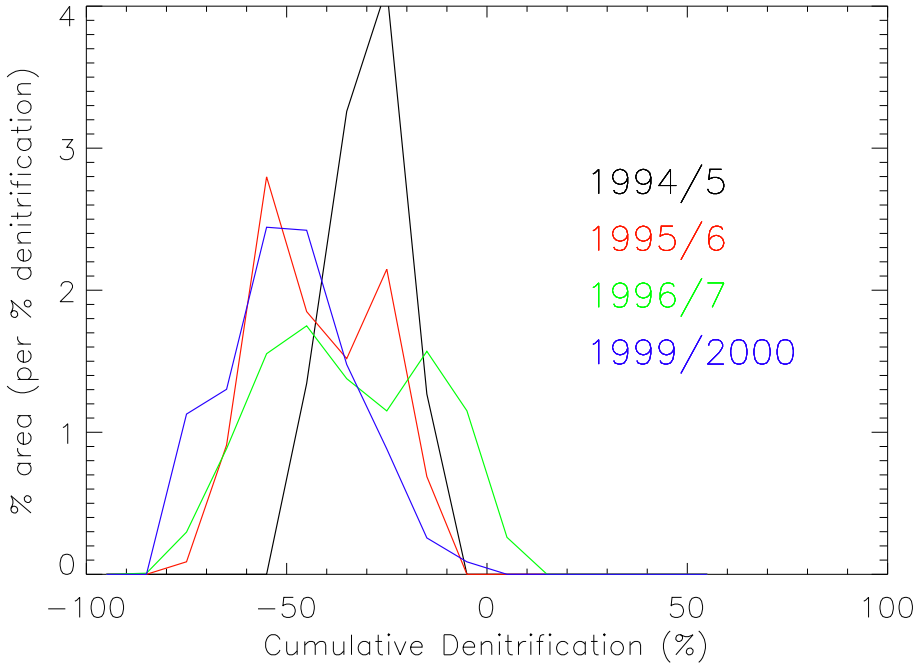

Fig. 5. Percentage area histograms of % denitrification at 465 K on 28 February of 1995, 1996, 1997 and 2000.

ACPD
2, 2557–2586, 2002

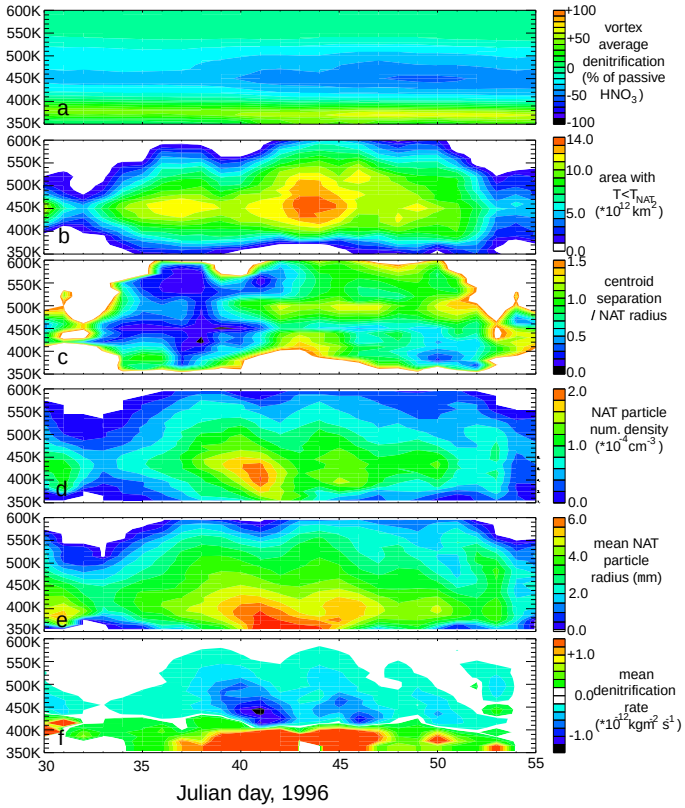

Fig. 6. Altitude time plots for February 1996 of **(a)** vortex average denitrification; **(b)** area of Arctic stratosphere below T_{NAT}; **(c)** normalized centroid separation; **(d)** particle number concentration; **(e)** mean particle radius; and **(f)** difference in incoming and outgoing downward NAT mass flux. Further details as in caption to Fig. 1. This figure shows more clearly the controlling influence of vortex/cold-pool concentricity on denitrification.

ACPD
2, 2557–2586, 2002

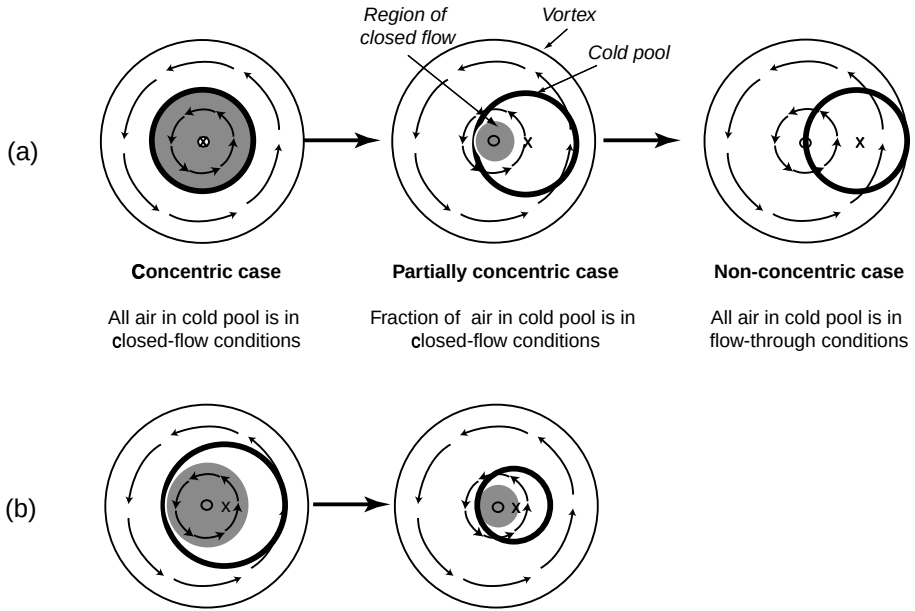

Fig. 7. Schematic of how the cold pool–vortex centroid separation and the cold pool area control the denitrification rate. The "closed-flow" region is shaded. **(a)** The effect of shifting the cold pool away from the centre of the vortex; **(b)** the effect of reducing the size of the cold pool.

ACPD
2, 2557–2586, 2002

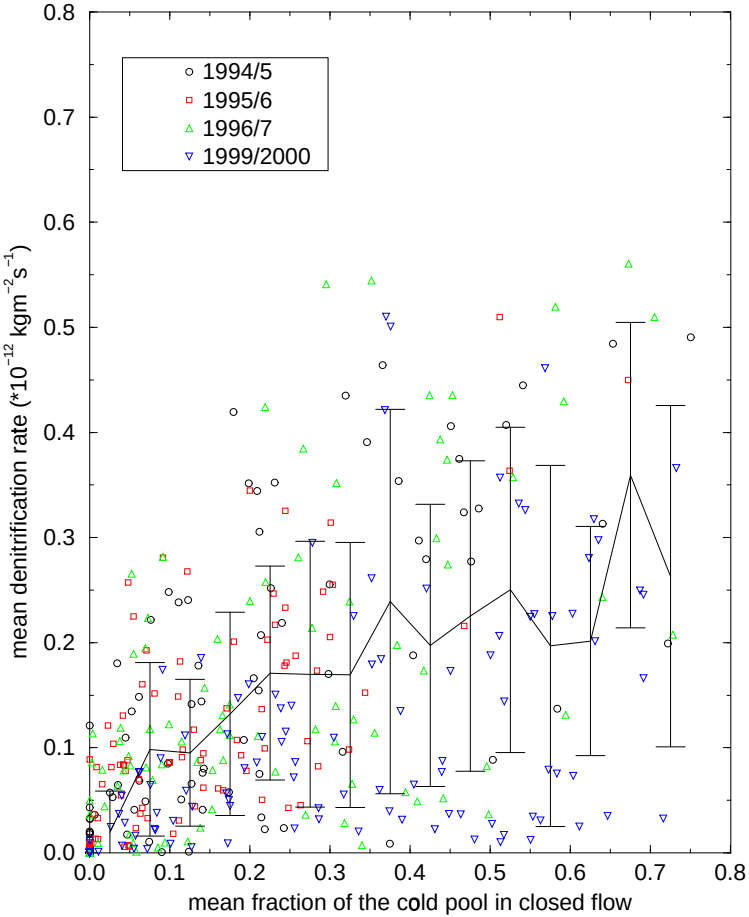

Fig. 8. The mean denitrification rate as a function of the mean fraction of the cold pool in which closed flow can occur. Details of the calculation of denitrification rate are given in Appendix B.

ACPD
2, 2557–2586, 2002